The Canadian Mineralogist
Vol. 55, pp. 29-44 (2017)
DOI: 10.3749/canmin.1600039

Re-Os SYSTEMATICS OF LÖLLINGITE AND ARSENOPYRITE IN GRANULITE-FACIES GARNET ROCKS: INSIGHTS INTO THE METAMORPHIC HISTORY AND THERMAL EVOLUTION OF THE BROKEN HILL BLOCK DURING THE EARLY MESOPROTEROZOIC (NEW SOUTH WALES, AUSTRALIA)

NICOLAS J. SAINTILAN[§]

Department of Earth and Atmospheric Sciences, University of Alberta, Edmonton, Alberta, T6G 2E3, Canada
Department of Earth Sciences, University of Durham, Durham DH1 3LE, UK

ROBERT A. CREASER

Department of Earth and Atmospheric Sciences, University of Alberta, Edmonton, Alberta, T6G 2E3, Canada

PAUL G. SPRY

Department of Geological and Atmospheric Sciences, 253 Science I, Iowa State University, Ames, Iowa, 50011-3212, U.S.A.

DANNY HNATYSHIN

Department of Earth and Atmospheric Sciences, University of Alberta, Edmonton, Alberta, T6G 2E3, Canada

ABSTRACT

Löllingite and arsenopyrite aggregates occur in spessartine-almandine garnet rocks (garnetite) metamorphosed to granulite facies, which are spatially associated with Pb-Zn-Ag mineralization in the giant Broken Hill deposit, southern Curnamona Province, New South Wales, Australia. Sulfarsenide and sulfide minerals comprise löllingite and coexisting arsenopyrite ± galena ± tetrahedrite that occur interstitial to garnet crystals. Löllingite formed first while gold-bearing löllingite, which occurs as rare relicts in arsenopyrite, was destroyed to produce arsenopyrite ± detectable micro-inclusions of invisible gold.

Standard mineral separation procedures produced pure separates of löllingite, arsenopyrite, and mixtures of arsenopyrite ± löllingite and löllingite ± arsenopyrite. In a plot of $^{187}Re/^{188}Os$ *versus* $^{187}Os/^{188}Os$, samples of löllingite and löllingite ± arsenopyrite have $^{187}Re/^{188}Os$ ratios between 6.87 and 7.40 and $^{187}Os/^{188}Os$ ratios between 0.8506 and 0.8651, whereas arsenopyrite and arsenopyrite ± löllingite samples have higher $^{187}Re/^{188}Os$ ratios (7.14 to 11.32) and more radiogenic $^{187}Os/^{188}Os$ ratios (0.8828 to 0.9654). Thirteen analyses of arsenopyrite and arsenopyrite ± löllingite define a Model 1 isochron with an age of 1574 ± 38 Ma (2σ; MSWD = 1.4, initial $^{187}Os/^{188}Os$ ratio of 0.666 ± 0.006), whereas the five löllingite and löllingite ± arsenopyrite samples define a Model 1 isochron with an age of 1707 ± 290 Ma (2σ; MSWD = 0.32, initial $^{187}Os/^{188}Os$ ratio of 0.652 ± 0.036) that is indistinguishable from the arsenopyrite age. Rhenium and Os contents are extremely high for löllingite and arsenopyrite (Re = 120–475 ppb; Os = 65–345 ppb), likely as a result of concentration of Re and Os in these minerals during granulite-facies metamorphism from the inferred exhalite protolith. Petrographic observations combined with the Model 1 Re-Os ages and literature SHRIMP U-Pb ages of monazite in garnetite suggest that arsenopyrite formed on the retrograde path at the expense of löllingite.

Cooling from peak Olarian *P-T* conditions (~800 °C at 1602 Ma) to at least 550 °C (first temperature of stability of arsenopyrite) at *ca*. 1574 Ma occurred at a rate of ~9 °C/Myr, which is similar to the rate of cooling determined for previously published SHRIMP U-Pb ages from successive monazite generations (McFarlane & Frost 2009). These results are consistent with the late phase of retrograde metamorphism that began between *ca*. 1590 and 1575 Ma.

Keywords: Re-Os, löllingite, arsenopyrite, gold, garnetite, Broken Hill, closing temperature, Olarian Orogeny.

[§] *Corresponding author e-mail address*: saintilanic@gmail.com

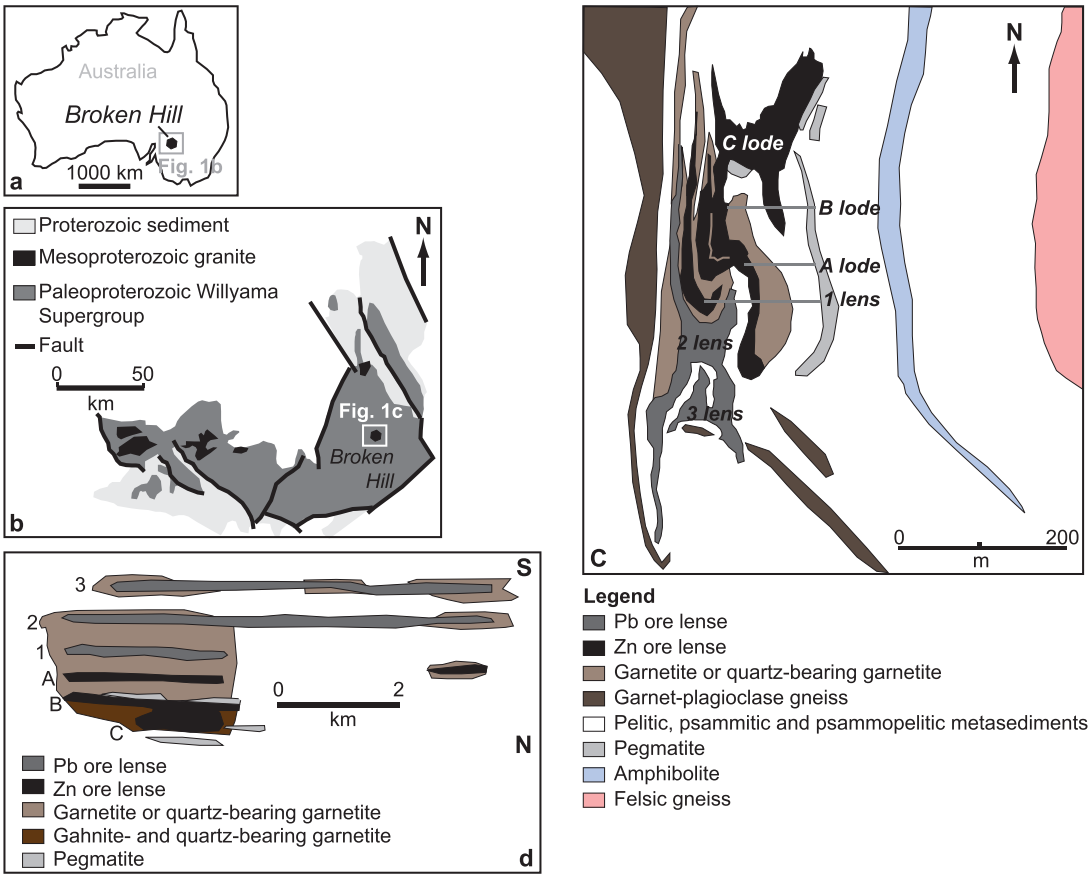

FIG. 1. (a) Location of the Broken Hill Zn-Pb-Ag deposit in New South Wales, Australia. (b) Regional geology in the Broken Hill area (after Plimer 2006). (c) Geology of the Broken Hill deposit (after Plimer 2006). (d) Schematic reconstruction in map view of the spatial relationship between garnet rocks, quartz-bearing garnet rocks, gahnite-bearing garnet rocks, and the different Zn or Pb ore lenses at the Broken Hill deposit (after Spry & Wonder 1989).

INTRODUCTION

Safflorite ($CoAs_2$), rammelsbergite ($NiAs_2$), and löllingite ($FeAs_2$) form a solid-solution series with estimated crystallization temperatures for these minerals between 550 and 625 °C (Raič *et al.* 2014). Löllingite occurs in high-grade metamorphosed (*i.e.*, amphibolite- to granulite-facies) sulfide deposits where it typically forms at the expense of arsenopyrite (FeAsS) through a loss of volatiles (*e.g.*, H_2S) during prograde metamorphism (Tomkins & Mavrogenes 2001, Davies *et al.* 2010). In pyrite-poor massive-sulfide deposits containing disseminated iron silicates or oxides, metamorphic processes lower $f(S_2)$ and promote the solid-state conversion of arsenopyrite to löllingite and pyrrhotite, rather than arsenopyrite melting (Pokrovski *et al.* 2002, Tomkins *et al.* 2006). Arsenopyrite may form at the expense of löllingite through addition of volatiles (*e.g.*, H_2S) and cooling during retrograde metamorphism (*e.g.*, Tomkins & Mavrogenes 2001).

Occurrences of disseminated löllingite and arsenopyrite crystals (hereafter referred to as "sulfarsenides") are reported in spessartine-almandine garnet rocks or "garnetite" metamorphosed to the granulite facies that are spatially associated with the Broken Hill Pb-Zn-Ag deposit, New South Wales, Australia (Fig. 1; Spry & Wonder 1989, Plimer 2006). Petrographic work by Spry (1978) and Plimer (2006) suggested that arsenopyrite in garnetite is the product of the breakdown of pre-existing löllingite during retrograde metamorphism.

The present work aims to determine an age for the sulfarsenides in garnetite using the Re-Os isotope system and processing individual löllingite and

arsenopyrite mineral separates. In an ideal case, distinct Re-Os ages for the prograde phase (precipitation of löllingite) and retrograde phase of metamorphism (precipitation of arsenopyrite) might be determined, and allow us to evaluate the conclusions of Spry (1978) and Plimer (2006) regarding the timing of formation of these minerals. In addition, by combining literature data on the temperature of precipitation and stability fields of löllingite and arsenopyrite with the obtained Re-Os ages, we may bring new insights into the metamorphic and thermal evolution (cooling rate?) of the Broken Hill block. The Re-Os data are compared to data obtained previously using the U-Th-Pb geochronometer in zircon and monazite, Sm-Nd geochronometer of garnet, and the Ar-Ar ages of hornblende, plagioclase, and clinopyroxene for the tectono-metamorphic and thermal events that affected garnetite and other Mesoproterozoic to Cambrian metamorphic rocks in the Broken Hill area (*e.g.*, Harrison & McDougall 1981, Ehlers *et al*. 1996, Page *et al*. 2005a, b).

Geological Background

The Broken Hill ore deposit occurs in metasedimentary rocks of the Paleoproterozoic Willyama Supergroup, which lie within the fault-bounded Broken Hill Domain of the Curnamona Craton (Fig. 1b). SHRIMP U-Pb geochronology using zircon constrains the age of the Willyama Supergroup at 1689 ± 5 to 1686 ± 3 Ma (1σ, Page *et al*. 2005a, b). The Willyama Supergroup is conformably overlain by the Sundown Group, which is younger than 1672 ± 7 Ma (Page *et al*. 2005a). The Broken Hill Domain is characterized by a regional prograde metamorphic pattern with amphibolite facies in the NW to granulite facies in the SE (Binns 1964, Phillips 1980, Phillips & Wall 1981). The Willyama Supergroup was subjected to at least three phases of deformation (D_1–D_3) associated with the Olarian Orogeny between 1657 and ~1575 Ma (*e.g.*, Page & Laing 1992, Page *et al*. 2005a, b, Forbes *et al*. 2008, McFarlane & Frost 2009). Folds associated with these deformation events are isoclinal (D_1), macroscopic tight with near-vertical axial planes (D_2), and near-vertical open with D_3 (Laing *et al*. 1978). Uranium-Pb zircon ages for D_2 and D_3 are indistinguishable and dated within the interval 1597 ± 3 to 1591± 5 Ma (Page *et al*. 2005a). Due to complexities of structural interpretation, a specific age for D_1 is uncertain, although it likely overlaps the older 1597 ± 3 Ma age given for the age interval for D_2–D_3 (Page *et al*. 2005a). Metamorphic conditions are slightly higher for D_1 than D_2 (Majoribanks *et al*. 1980, Frost *et al*. 2005) with peak conditions of ~780 °C and ~5.2 kbar (Phillips 1980, Phillips & Wall 1981) affecting the Broken Hill deposit. Retrograde metamorphism ($T = 550$ to 600 °C, $P = 5$ to 5.5 kbar; Phillips 1980, Corbett & Phillips 1981, Stevens 1986) began during D_3 and is associated with initiation of retrograde shear zones that occur throughout the Broken Hill area and cross-cut the Broken Hill deposit. This retrograde history is supported by ^{40}Ar-^{39}Ar cooling ages (hornblende, clinopyroxene, muscovite) in the range of 1550 to 1500 Ma, suggesting that the area cooled down to and below 500 °C at a rate of ~3 °C/Myr between 1660 and 1570 Ma (Harrison & McDougall 1981). Following granitoid emplacement at *ca*. 1500 Ma, the region remained below 350 °C until a thermal event affected the Curnamona Province during the Delamerian orogeny in early Paleozoic time (Harrison & McDougall 1981). Retrograde regional shear zones in Paleoproterozoic basement rocks of the Curnamona Province comprise greenschist- to amphibolite-grade mineral assemblages that formed between 517 and 497 Ma (Dutch *et al*. 2005). The pressure-temperature conditions calculated from the garnet-staurolite-biotite-muscovite-chlorite-quartz-bearing mineral assemblages in the shear fabrics are between 530 and 600 °C at *ca*. 5 kbar (Dutch *et al*. 2005) whereas Harrison & McDougall (1981) suggested that temperatures only locally reached ~350 °C at 520 ± 40 Ma (Rb-Sr, biotite; ^{40}Ar-^{39}Ar, plagioclase).

The Broken Hill ore deposit within the Broken Hill domain comprises six stacked orebodies that were metamorphosed to the granulite facies and affected by large, recumbent, isoclinal D_2 folds (Fig. 1c; Plimer 2006). The orebodies are spatially associated with three types of garnet-rich rock (quartz garnetite, garnetite, and so-called "garnet envelope"), which are described in detail by Spry & Wonder (1989), Plimer (2006), and Spry *et al*. (2007); the descriptions are not repeated here (Fig. 1c–d). It should be noted that garnet envelope occurs on the margins of the Pb-rich orebodies as garnet stringers discordant to S_0 and S_1, generally parallel to S_3, or where garnet surrounds veins that cross-cut quartz garnetite (Spry & Wonder 1989). Garnetite contains >80% garnet along with various accessory minerals (*e.g.*, quartz, plagioclase, gahnite, sulfides, sulfosalts, arsenides, sulfarsenides) as tabulated in Spry & Wonder (1989, their Table 2). In places, blue quartz-bearing garnetite contains euhedral to subhedral arsenopyrite crystals up to 0.5 cm in length (Fig. 2a). Garnetite occurs mostly on the margins of lenses 1, 2, and 3 and the A lode, as inclusions in mineralization, and along strike from sulfide mineralization. Plimer (2006) and Spry *et al*. (2007) describe laminations in garnetite that mainly parallel bedding and the S_1 schistosity (the axial plane schistosity of F_1 folds). However, in places, the garnetite is chaotically folded and unrelated to S_1. The

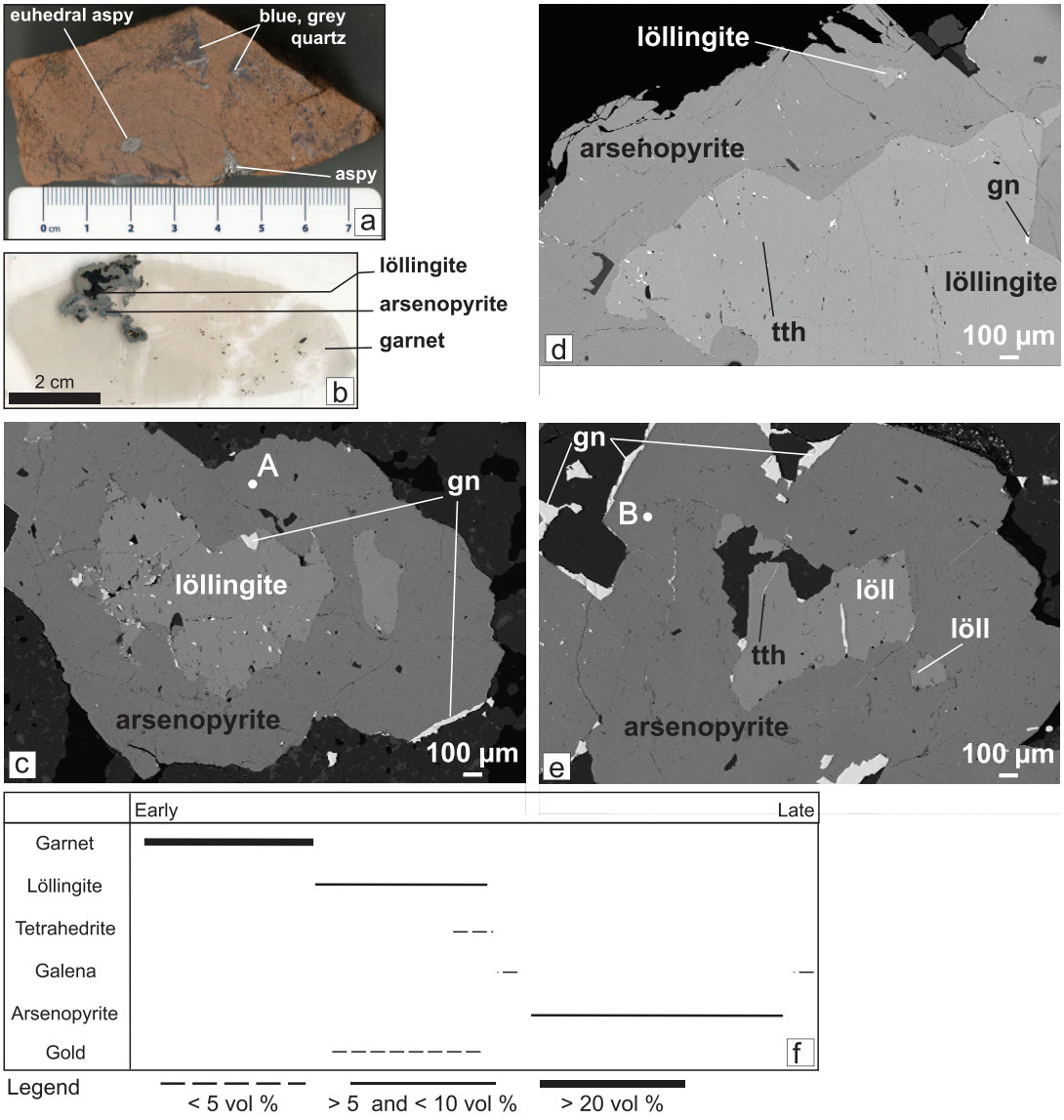

FIG. 2. (a) Polished slab of the sulfide-bearing spessartine-almandine sample utilized for Re-Os isotope geochemistry. Euhedral arsenopyrite is embedded in garnets. Anhedral arsenopyrite masses are also present. (b) Polished thin section of this slab showing sulfide aggregates composed of a core of löllingite irregularly surrounded by arsenopyrite. Some grains of galena (white grains) are seen at the contact between löllingite and arsenopyrite. (c, d, e) SEM-BSE images of arsenopyrite-löllingite mineralization. Two phases of galena (gn) precipitation are recorded. Tetrahedrite (tth) fills fractures in löllingite but not in arsenopyrite. In (b) and (c), SEM-BSE images complemented by SEM-EDS analyses identified "invisible gold" in arsenopyrite (Point A at 2.0 wt.% Au, Point B at 4.8 wt.% Au; see text for further details). (f) Paragenetic sequence of the sample.

origin of garnetite is controversial and is centered on three main proposals: (1) metamorphism of manganiferous sediments (*e.g.*, Wright *et al.* 1987, Spry & Wonder 1989, Lottermoser 1989, Plimer 2006, Spry *et al.* 2007); (2) metasomatic mobilization of Mn between the sulfide lenses and the wall rocks either syn- (D_1–D_2) or post-peak metamorphism (D_3) (Hodgson,1975, Prendergast *et al.* 1998); (3) reaction of Mn derived from partially melted sulfide orebodies with the surrounding pelitic gneisses (Frost *et al.* 2002, Sparks

& Mavrogenes 2003). It should be noted that Plimer (2006) proposed that garnetite formed as a result of possible retrograde metamorphic reactions fostered by the rheological contrast between galena-rich sulfide orebodies and the enclosing metamorphic silicate rocks. Preliminary U-Pb zircon ages and Sm-Nd garnet ages for garnetite yielded "a metamorphic age of around 1590 Ma" (Ehlers *et al*. 1996). Regardless of the origin of garnetite, it is clear that it is a metamorphic rock that was subjected to granulite-facies metamorphism during the Olarian orogeny and to a Cambrian thermal event during the Delamarian orogeny.

Methodology

Relationships between arsenopyrite and löllingite were studied by means of optical and scanning-electron microscope (SEM) using a representative polished thin section from garnetite sample "532-35", containing arsenopyrite (Figs. 2a, b), from between the 1 and 2 lenses on the 21 level of the old New Broken Hill Consolidated Mine at the southern end of the Broken Hill deposit (Fig. 1c). A Zeiss Sigma 300 Field Emission SEM (VP-FESEM) was operated in back-scattered electron mode (SEM-BSE, beam conditions of 15 kV). A Bruker energy-dispersive X-ray spectroscopy (EDS) system with dual silicon drift detectors, each with an area of 60 mm^2 and a resolution of 123 eV, was used for single-spot analysis.

Sample 532-35 was cut into slabs that were thoroughly cleaned using silicon carbide grit and paper to remove any metal traces left by hammering or sawing. The sample was crushed using an agate mortar and pestle and sieved through disposable home-made nylon sieves to produce 70–200 and +70 mesh size fractions. These fractions were treated by standard heavy liquid separation and arsenopyrite and löllingite were extracted by magnetic concentration using a Frantz Isodynamic Separator to produce magnetic (M) and non-magnetic (NM) fractions by applying successive 1.7 and 2.2 amp currents with 15° side slope and 10° forward slope, and 2° side slope and 10° forward slope for these currents, respectively. A fraction is thus always referred to as follows: "mesh size, magnetic property, and side slope/forward slope". The composition of each mineral separate was determined by X-ray diffraction (XRD) analysis and visually assessed by SEM-BSE images complemented by qualitative SEM-EDX analysis (Table 1).

For each Re-Os analysis, between 12 and 36 mg of arsenopyrite or löllingite mineral separates were weighed and transferred into thick-walled borosilicate Carius tubes. Each sample was dissolved in inverse aqua regia (~2 mL of 10 N HCl and ~6 mL 16 N HNO_3) with a known amount of $^{185}Re + {}^{190}Os$ spike solution at 220 °C for 24 hours. The full Re-Os laboratory protocol used in the present study is given in Hnatyshin *et al*. (2016). Rhenium and Os isotopic compositions were determined by negative thermal ionization mass spectrometry (NTIMS; Creaser *et al*. 1991, Völkening *et al*. 1991) using a ThermoScientific Triton mass spectrometer at the Canadian Centre for Isotopic Microanalysis, University of Alberta, Edmonton, Canada. Rhenium was measured as ReO_4^- in static mode with Faraday collectors, whereas Os was measured as OsO_3^- in peak-hopping mode with the SEM and a constant flow of oxygen (Creaser *et al*. 1991, Völkening *et al*. 1991). Total procedural blanks returned the following values [Batch #1, $n = 3$ procedural blanks, for samples UA-01-BHA to UA-14-BHA, Re = 4.4 ± 0.98 pg (1σ), Os = 1.34 ± 0.03 pg (1σ), blank $^{187}Os/^{188}Os = 0.27$; Batch #2 for samples UA-15-BHA to UA-18-BHA, Re = 2.3 ± 0.47 pg (1σ), Os = 0.08 ± 0.05 pg (1σ), blank $^{187}Os/^{188}Os = 0.80$]. Measurement quality was monitored by repeated measurements of in-house Re (natural Re, $^{185}Re/^{187}Re = 0.59774 \pm 0.00065$, $n = 23$) and Os (AB-2, $^{187}Os/^{188}Os = 0.10682 \pm 0.00009$, $n = 100$) standard solutions. Rhenium analyses are corrected for isobaric oxide interferences, and normalized to a value of 0.5974 based on long-term measurements of the Re standard. Raw OsO_3^- ratios were corrected for isobaric oxides interferences, spike contribution, and mass fractionation using a $^{192}Os/^{188}Os$ value of 3.08261 using an exponential law (Hnatyshin *et al*. 2016). Isochron regression of the Re-Os data was performed using Isoplot v. 4.15 (Ludwig 2011) and the ^{187}Re constant of Smoliar *et al*. (1996).

TABLE 1. ELEMENTAL COMPOSITION OF LÖLLINGITE AND ARSENOPYRITE AS DETERMINED BY QUALITATIVE SEM-EDX ANALYSES (ERROR: ± 10%)

löllingite ($n = 31$)	S wt.%	Fe wt.%	Co wt.%	Ni wt.%	As wt.%
average	1.3	18.8	4.0	2.0	74.0
standard deviation	0.3	1.4	0.7	0.4	1.4
arsenopyrite ($n = 30$)	**S wt.%**	**Fe wt.%**	**Co wt.%**	**Ni wt.%**	**As wt.%**
average	16.9	30.3	2.1	0.1	50.6
standard deviation	0.9	2.0	1.0	0.2	2.2

Results

Petrography

In hand specimen, aggregates of arsenopyrite and löllingite occur interstitially to garnets (Figs. 2a, b). Arsenopyrite occurs locally as euhedral crystals up to

0.5 cm in diameter (Figs. 2a, b), but it also occurs as disseminations along with löllingite throughout the rock as anhedral aggregates. Each aggregate shows a core of black löllingite that is irregularly rimmed by grey arsenopyrite (Fig. 2b). Galena is visible in hand specimen at the contact between these two phases.

The SEM-BSE images show irregular contacts between löllingite and arsenopyrite and inclusions of löllingite in arsenopyrite (Fig. 2c, d, e). Fractures present in the löllingite were filled in by tetrahedrite. These fractures are not visible in arsenopyrite and must predate its formation. Hence, löllingite ± tetrahedrite predates the formation of arsenopyrite (Fig. 2f). Galena formed after löllingite ± tetrahedrite and as late rims on arsenopyrite or filling fractures in arsenopyrite. In some rare instances, small inclusions (<10 μm) of arsenopyrite occur in löllingite and might indicate that arsenopyrite was present prior to löllingite precipitation. Alternatively, these inclusions might be local replacement of löllingite by arsenopyrite, as it appears to be the most common texture in the studied sample.

These petrographic observations were complemented by SEM-EDX analyses of löllingite and arsenopyrite (average values in Table 1, full data set available as Electronic Supplementary Material 1). In sample 532-25, qualitative analyses of löllingite shows that it contains an average of 4.0 wt.% Co, 2.0 wt.% Ni, and 1.3 wt.% S, whereas arsenopyrite contains lower amounts of Co (~2.1 wt.%) and Ni (~0.1 wt.%). Unobservable but detectable gold, which is referred to as "invisible gold" (*cf.* Tomkins & Mavrogenes 2001), was identified through single-spot SEM-EDX analyses as disseminated micro-inclusions in arsenopyrite (*e.g.*, Fig. 2c, e, Point A = 2.0 wt.% Au; Fig. 2e, Point B = 4.8 wt.% Au).

Mineral separates and XRD data

Five magnetic and non-magnetic fractions were obtained during sample processing (Table 2). All fractions correspond to sulfarsenides with trace amounts of galena or tetrahedrite as verified by XRD analyses. The purity of these mineral fractions was assessed by means of SEM-BSE images and XRD analyses (Fig. 3). Three fractions correspond to 100% pure monomineral fractions of arsenopyrite or löllingite: (1) the "70–200, NM 2.2, 2/10" and "+70, NM 2.2, 2/10" fractions containing arsenopyrite (Fig. 3a) and (2) the "70–200, M 1.7, 15/10" fraction containing Co-rich löllingite (Fig. 3b). The two remaining fractions correspond to mixtures of these sulfarsenides in different proportions: (1) the "+70, M 1.7, 15/10" fraction corresponding to 80–100% löllingite and 0–20% arsenopyrite (Fig. 3c) and (2) the "+70, M 2.2., 2/10" fraction corresponding to 70–100% arsenopyrite and 0–30% löllingite (Fig. 3d).

Re-Os isotope geochemistry

The results of 18 Re-Os isotope analyses of the sulfarsenide mineral separates are presented in Table 2. These data reveal Re contents systematically higher than 120 ppb in both löllingite and arsenopyrite and two overlapping ranges of Re contents depending on the type of sulfarsenide mineral: (1) between 120 and 385 ppb Re in arsenopyrite and (2) between 300 and 475 ppb Re in löllingite. Osmium concentrations are also very high (>63 ppb) in these sulfarsenides. The löllingite and löllingite ± arsenopyrite samples have the highest total Os contents (222 to 346 ppb), whereas the arsenopyrite and arsenopyrite ± löllingite samples have lower total Os contents (64 to 255 ppb). Uncertainties (±2σ) are 0.36% or better for Re abundances and 0.26% or better for Os. The variation in total Re (and corresponding radiogenic $^{187}Os^*$) and common ^{192}Os contents between the sulfarsenide minerals resulted in a relatively narrow range of low $^{187}Re/^{188}Os$ and low radiogenic $^{187}Os/^{188}Os$ ratios. Löllingite and löllingite ± arsenopyrite samples plot in the bottom left-hand corner of the $^{187}Re/^{188}Os$ *versus* $^{187}Os/^{188}Os$ plot with $^{187}Re/^{188}Os$ ratios between 6.87 and 7.40 and $^{187}Os/^{188}Os$ ratios between 0.8506 and 0.8651, whereas the arsenopyrite and arsenopyrite ± löllingite samples have higher $^{187}Re/^{188}Os$ ratios (7.14 to 11.32) and more radiogenic $^{187}Os/^{188}Os$ ratios (0.8828 to 0.9654; Fig. 4a).

On a conventional $^{187}Re/^{188}Os$ *versus* $^{187}Os/^{188}Os$ plot, the 13 arsenopyrite and arsenopyrite ± löllingite samples define a Model 1 isochron with an age of 1574 ± 38 Ma (Fig. 4b; 2σ; mean squared weighted deviates, MSWD = 1.4, initial $^{187}Os/^{188}Os$ ratio [Os]i = 0.666 ± 0.006). Despite the small range of $^{187}Re/^{188}Os$ ratios (~7 to ~12), the fit of data to the regression line yields a 2σ age uncertainty of only ± 2.4%. The five löllingite and löllingite ± arsenopyrite samples define a Model 1 isochron with an age of 1707 ± 290 Ma (Fig. 4c; 2σ; MSWD = 0.32, initial $^{187}Os/^{188}Os$ ratio [Os]i = 0.652 ± 0.036). Given the narrow spread of $^{187}Re/^{188}Os$ ratios (~6.8 to ~7.8), the fit of data to the regression line yields a large 2σ age uncertainty of ~17%. This age and its original Os ratio overlap within error with the age and original Os ratio defined by the arsenopyrite samples.

Discussion

Relative chronology between löllingite and arsenopyrite and invisible gold in arsenopyrite

Our petrographic observations of irregular contacts between löllingite and arsenopyrite and relicts of löllingite in arsenopyrite crystals (Fig. 2c–e) are similar to the textures observed by Tomkins &

TABLE 2. MINERAL COMPOSITION, MAGNETIC SUSCEPTIBILITY AND FRANTZ FRACTION, AND Re-Os ISOTOPIC DATA OF ALIQUOTS FROM ARSENOPYRITE AND LÖLLINGITE IN SPESSARTINE-ALMANDINE GARNETITE FROM THE BROKEN HILL DEPOSIT

Sample	Frantz magnetic fraction	Mineralogy (XRD data and SEM images)	Weight (mg)	Re (ppb)	± 2σ	Total Os (ppt)	± 2σ	$^{187}Re/^{188}Os$	± 2σ	$^{187}Os/^{188}Os$	± 2σ	rho	% Re blank	$\%^{187}Os$ blank	$\%^{188}Os$ blank
UA-05-BHA	+70, M 2.2, 2/10	arsenopyrite ± löllingite	20.86	133.6	0.5	63919	181	11.17	0.04	0.9628	0.0034	0.454	0.02	0.009	0.030
UA-09-BHA	+70, M 2.2, 2/10	arsenopyrite ± löllingite	27.49	382.5	1.4	254782	701	7.94	0.03	0.8791	0.0031	0.459	0.01	0.002	0.006
UA-12-BHA	+70, M 2.2, 2/10	arsenopyrite ± löllingite	24.81	142.9	0.5	105605	287	7.14	0.03	0.8574	0.0030	0.461	0.02	0.005	0.015
UA-06-BHA	+70, NM 2.2, 2/10	arsenopyrite	20.31	320.2	1.2	194463	537	8.73	0.03	0.8977	0.0032	0.461	0.01	0.003	0.010
UA-10-BHA	+70, NM 2.2, 2/10	arsenopyrite	20.85	209.0	0.8	117826	332	9.43	0.03	0.9165	0.0033	0.451	0.02	0.005	0.016
UA-11-BHA	+70, NM 2.2, 2/10	arsenopyrite	20.16	239.4	0.9	151940	415	8.34	0.03	0.8875	0.0031	0.458	0.01	0.004	0.013
UA-13-BHA	+70, NM 2.2, 2/10	arsenopyrite	36.20	246.4	0.9	116388	329	11.32	0.04	0.9654	0.0034	0.460	0.01	0.003	0.009
UA-14-BHA	+70, NM 2.2, 2/10	arsenopyrite	32.00	121.3	0.4	69525	198	9.27	0.03	0.9130	0.0034	0.459	0.02	0.005	0.018
UA-15-BHA	+70, NM 2.2, 2/10	arsenopyrite	20.60	159.1	0.5	85410	240	9.92	0.03	0.9315	0.0033	0.539	0.07	0.004	0.005
UA-16-BHA	+70, NM 2.2, 2/10	arsenopyrite	12.92	140.3	0.4	75147	217	9.94	0.03	0.9334	0.0035	0.529	0.13	0.007	0.008
UA-17-BHA	+70, NM 2.2, 2/10	arsenopyrite	16.83	146.8	0.5	70767	237	11.09	0.04	0.9633	0.0045	0.540	0.09	0.006	0.007
UA-04-BHA	70-200, NM 2.2, 2/10	arsenopyrite	20.91	174.5	0.6	106192	296	8.71	0.03	0.8949	0.0032	0.458	0.02	0.006	0.018
UA-08-BHA	70-200, NM 2.2, 2/10	arsenopyrite	21.41	225.1	0.8	145315	397	8.20	0.03	0.8828	0.0031	0.460	0.01	0.004	0.013
UA-01-BHA	70-200, M 1.7, 15/10	löllingite	10.86	473.4	1.7	345733	950	7.23	0.03	0.8607	0.0031	0.464	0.01	0.003	0.010
UA-03-BHA	70-200, M 1.7, 15/10	löllingite	14.33	397.0	1.4	304605	809	6.87	0.03	0.8506	0.0029	0.459	0.01	0.003	0.009
UA-18-BHA	+70, M 1.7, 15/10	löllingite ± arsenopyrite	14.46	318.5	1.0	222444	603	7.57	0.02	0.8707	0.0030	0.539	0.05	0.002	0.002
UA-02-BHA	+70, M 1.7, 15/10	löllingite ± arsenopyrite	12.69	449.8	1.6	332046	907	7.15	0.03	0.8570	0.0031	0.459	0.01	0.003	0.009
UA-07-BHA	+70, M 1.7, 15/10	löllingite ± arsenopyrite	13.46	392.1	1.4	279816	753	7.40	0.03	0.8651	0.0030	0.461	0.01	0.003	0.010

Note: +70 and 70–200 are the mesh size fractions, M: Magnetic at x, NM: non-magnetic at x, x = current in amps, (y°/z°) = (side slope/forward slope).

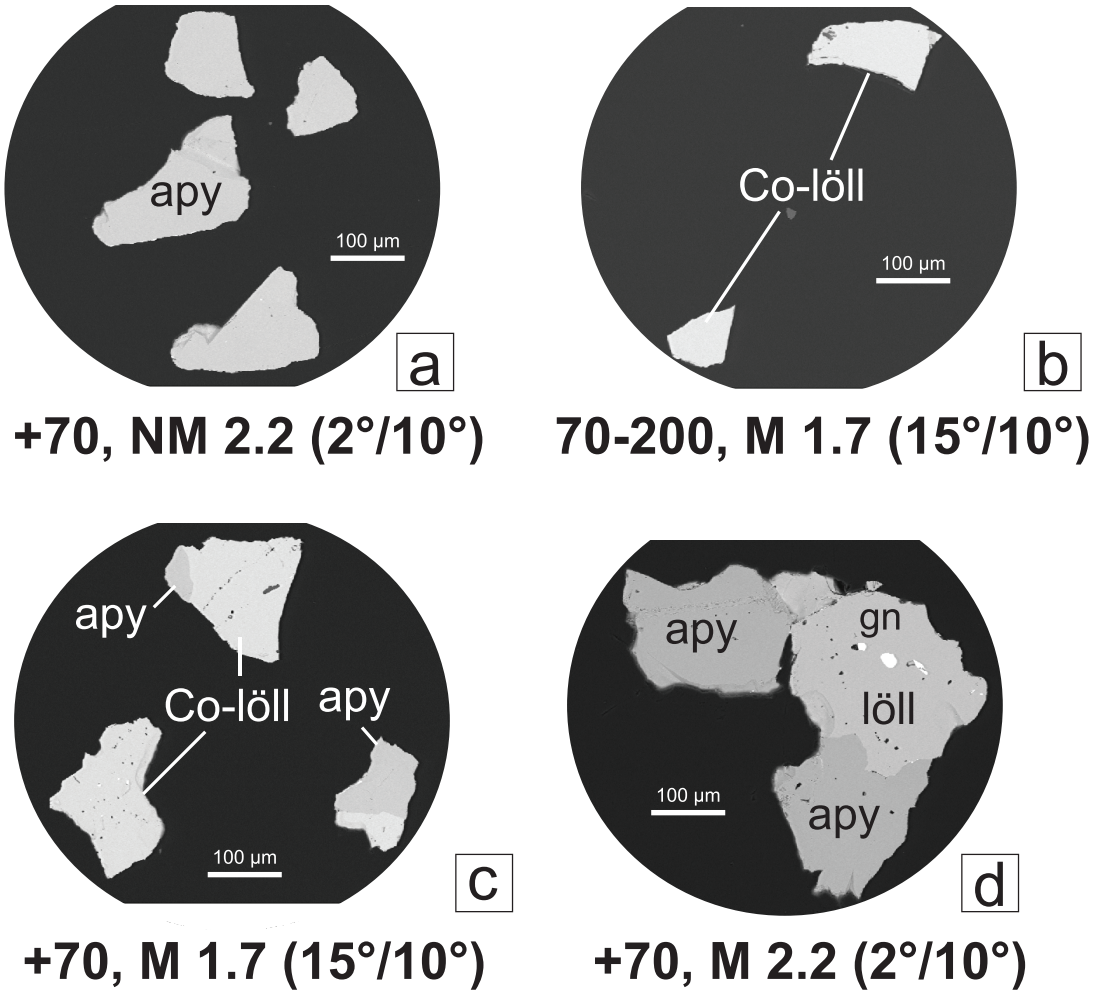

FIG. 3. Scanning electron microscope images in backscattered mode (SEM-BSE) of mineral separates mounted in epoxy. (a) +70 mesh, magnetic fraction at 2.2 amps, side slope at 2°/forward slope at 10°. (b) 70–200 mesh, magnetic fraction at 1.7 amps, side slope at 15°/forward slope at 10°. (c) +70 mesh, magnetic fraction at 1.7 amps, side slope at 15°/forward slope at 10°. (d) +70 mesh, magnetic fraction at 2.2 amps, side slope at 2°/forward slope at 10°. Abbreviations: apy: arsenopyrite, gn: galena, löll: löllingite, Co-löll: Co-rich löllingite (Co >3 wt.%, SEM-EDX).

Mavrogenes (2001; their Fig. 5c) for the formation of arsenopyrite at the expense of löllingite during retrograde metamorphism (Fig. 2f). Consequently, arsenopyrite and löllingite are in petrographic disequilibrium. Tomkins & Mavrogenes (2001) suggested that this texture is also diagnostic of the original complete prograde metamorphism of arsenopyrite to löllingite. The only evidence in favor of this interpretation in our case are the rare blebs of arsenopyrite (<10 µm) that are tentatively interpreted as relicts of arsenopyrite that were metamorphosed during a prograde phase.

The destruction of löllingite during retrograde metamorphism would explain the presence of trace Co and Ni and their uneven distribution in arsenopyrite (Table 1). In addition, the detection of invisible gold in arsenopyrite is a feature that can be explained by the destruction of löllingite and the redistribution of gold during retrograde metamorphism (*cf.* Tomkins & Mavrogenes 2001). Indeed, desulfidation

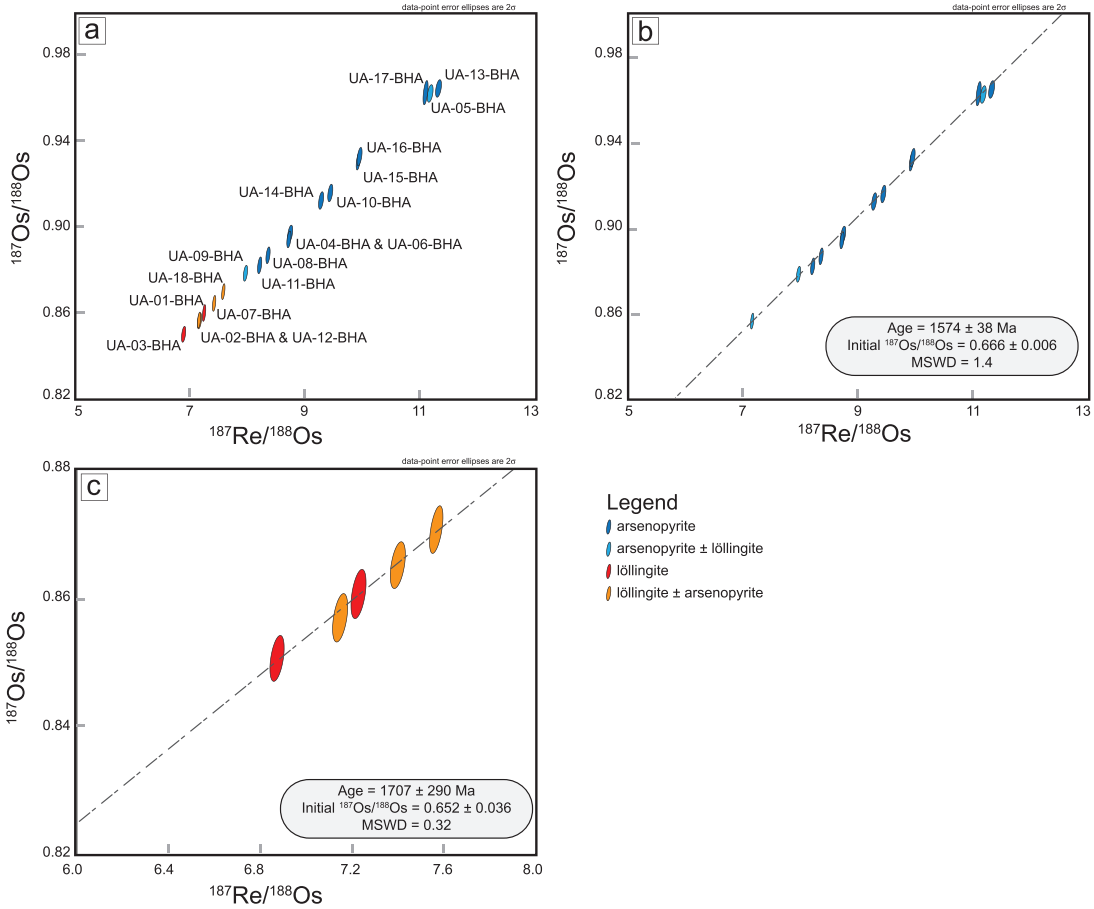

FIG. 4. (a) Re-Os isotope geochemistry data points for arsenopyrite, arsenopyrite ± löllingite, löllingite, and löllingite ± arsenopyrite with error ellipses in the $^{187}Os/^{188}Os$ *versus* $^{187}Re/^{188}Os$ space. (b) Isochron regression diagram of the 13 Re-Os data points of arsenopyrite and arsenopyrite ± löllingite. (c) Isochron regression diagram of the five Re-Os data points for löllingite and löllingite ± arsenopyrite.

of a gold-sulfur complex under metamorphic conditions lower than granulite facies could result in the co-precipitation of arsenopyrite, löllingite, pyrrhotite, and native gold. In addition, arsenopyrite, löllingite, and pyrrhotite would not necessarily be in close spatial association. In the current study, the absence of pyrrhotite in the observed sulfarsenide aggregates, the relicts of löllingite in arsenopyrite, and the presence of native gold disseminated in arsenopyrite are favorable arguments to support the mechanism presented for post-peak metamorphic gold presence in arsenopyrite by Tomkins & Mavrogenes (2001). This conclusion is supported further by the absolute Re-Os age determination interpreted in the following section.

Significance of the Re-Os age in sulfarsenides and insights into the thermal evolution of the Broken Hill area during the Early Mesoproterozoic

The Re-Os age of 1574 ± 38 Ma recorded by the Re-Os isotopic system in arsenopyrite represents the time at which the Re-Os isotopic system was closed in arsenopyrite. The imprecise age recorded by the Re-Os isotopic system in löllingite overlaps within error the age defined by the arsenopyrite data points. Our petrographic observations show that löllingite and arsenopyrite are in petrographic disequilibrium, but the Re-Os isotope data are not sufficient to determine when löllingite formed prior to its partial destruction to arsenopyrite during retrograde metamorphism at *ca.*

TABLE 3. SUMMARY OF METAMORPHIC AND THERMAL EVENTS IN THE BROKEN HILL BLOCK, CURNAMONA CRATON FROM THE LATE PALEOPROTEROZOIC TO THE CAMBRIAN

Age (Ma)	Orogeny	Metamorphic event/grade	*T* (°C), *P* (kbar)	Mineral (Method)	Reference
1657 ± 8	Static?	lower amphibolite facies	<550?, <3?	monazite (U-Pb)	McFarlane & Frost (2009)
1630 ± 6	Olarian orogeny	upper amphibolite facies (prograde)	>650, 3–4	monazite (U-Pb)	McFarlane & Frost (2009)
1602 ± 9	Olarian orogeny	granulite facies (peak)	~800, 5–6	monazite (U-Pb)	McFarlane & Frost (2009)
1590–1575	Olarian orogeny	(retrograde)	< 650, ~5	monazite (U-Pb)	McFarlane & Frost (2009)
1660–1570	Olarian orogeny	prograde to retrograde	Cooling, below 500 °C after 1500 Ma, rate ~3 °C/Myr	hornblende, plagioclase, clinopyroxene (^{40}Ar-^{39}Ar)	Harrison & McDougall (1981)
1574 ± 38	Late Olarian orogeny?	(retrograde)	Cooling from peak Olarian conditions to at least 550 °C at a rate of ~9 °C/Myr	arsenopyrite (Re-Os)	This study
517–497	Delamerian orogeny	garnet-staurolite-biotite-muscovite-chlorite-quartz	530–600, ~5 (located in shear zones)	monazite, garnet (U-Pb, Sm-Nd)	Dutch *et al.* (2005)
520 ± 40	Delamerian orogeny		~350	biotite (Rb-Sr)	Harrison & McDougall (1981)

1574 Ma. Indeed, according to the summary of known metamorphic and thermal events that affected the Broken Hill Block in the Curnamona Craton (Table 3), the Re-Os age of arsenopyrite indicates that it formed during retrograde metamorphism affecting the garnetite that is proposed to have started from *ca*. 1590 to 1575 Ma (*cf*. McFarlane & Frost 2009). Our isotope geochemistry results are consistent with the interpretation of Spry (1978), who had determined that the cores of arsenopyrite, where intergrown with pyrrhotite, have high As:S ratios relative to the rims. He concluded that this pattern was diagnostic of the growth of arsenopyrite during retrograde metamorphism, as based on the studies of Kretschmar & Scott (1976) and Sharp *et al*. (1985).

McFarlane & Frost (2009) proposed that the SHRIMP *ca*. 1575 Ma U-Pb age recorded in their youngest monazite grains corresponds to the timing of final cooling of the rocks of the Broken Hill Block below minimum granitic melt temperatures of *ca*. 650 °C at a rate of ~10 °C/Myr. According to the experiments of Sharp *et al*. (1985), the use of the arsenopyrite geothermometer in our Broken Hill sample is precluded because this geothermometer yields an underestimation of the actual temperature of mineral precipitation for deposits metamorphosed to upper amphibolite and granulite facies. This underestimation is even more significant considering the trace-element contents of arsenopyrite in our sample (2.1 wt.% Co and 0.1 wt.% Ni in arsenopyrite, EDX analyses, this study; arsenopyrite containing up to 3.19 wt.% Co, 0.49 wt.% Ni, $n = 51$, microprobe analyses in Spry 1978). However, given the fact that arsenopyrite is stable at temperatures in the range 400 to 550 °C (Pokrovski *et al*. 2002, Tomkins *et al*. 2006, Raič *et al*. 2014), we may use 550 °C as the minimum temperature for the precipitation of arsenopyrite. Thus, cooling from peak Olarian *P–T* conditions (~800 °C at 1602 Ma; McFarlane & Frost 2009) to at least 550 °C at *ca*. 1574 Ma occurred at a rate of ~9 °C/Myr, *i.e*., a similar value to that determined by McFarlane & Frost (2009) using SHRIMP U-Pb ages of successive monazite generations. These results are also consistent with the timing of the closure of the Sm-Nd system in metamorphic garnet (600 ± 30 °C; Mezger *et al*. 1992) that occurred at 1580 Ma (Hand *et al*. 2003).

Löllingite forms at temperatures between 625 and 550 °C, whereas the destruction of löllingite to form arsenopyrite occurs when the temperature goes below 550 °C and enters the stability field of arsenopyrite (Pokrovski *et al*. 2002, Tomkins *et al*. 2006, Raič *et al*. 2014). Tomkins & Mavrogenes (2002) reported pre- to syn-peak metamorphic conditions in granulite-hosted gold deposits (*e.g*., Challenger and Griffin Find) in which löllingite survived temperatures of 700 to 850

°C and pressures of ~6 to 7.5 kbars. Considering the thermal constraints presented above for the retrograde cooling path for Broken Hill and the summary of events for both the prograde and retrograde paths in Table 3, our Re-Os age of 1707 ± 290 Ma suggests two possible scenarios for the formation of löllingite: (1) between *ca*. 1657 Ma and *ca*. 1630 Ma when *T* was between 550 and 650 °C prior to peak metamorphic conditions of ~800 °C at *ca*. 1602 Ma; or, alternatively, (2) after *ca*. 1580 Ma when temperatures went below 600 ± 30 °C. At the current state of knowledge, we cannot choose between these hypotheses.

Regional implications and evolution of the Broken Hill area compared to the Mount Isa Block during the Early Mesoproterozoic

Stratigraphic rationalization and SHRIMP U-Pb geochronology carried out in the eastern Mount Isa Block and the Curnamona Province, in complement to the original lithologic, metamorphic, and metallogenic similarities recognized in these terranes (Vaughan & Stanton 1984, Laing & Beardsmore 1986), support a strong correlation over the interval *ca*. 1710 to 1580 Ma between these terranes from deposition of the Willyama Supergroup (Curnamona Province) and Maronan Supergroup (eastern Mount Isa Block) to the initial stages of the Olarian (Curnamona Province) and Isan (eastern Mount Isa Block) orogenies (Giles *et al*. 2004). These authors included the Mount Isa block and the Curnamona Province within the same *ca*. 1600 to 1500 Ma orogenic belt (*cf*. their Fig. 4) and a late phase of thick-skinned deformation and crustal shortening was identified for the Isan orogeny at *ca*. 1550 to 1500 Ma (MacCready *et al*. 1998). In particular, two metamorphic events, which affected the Western Fold Belt of the Mount Isa Inlier, were identified at *ca*. 1575 Ma (Hand & Rubatto 2002) and 1532 ± 7 Ma, the latter of which was associated with the emplacement of pegmatite (Connors & Page 1995). Our Re-Os age of *ca*. 1574 Ma for the formation of arsenopyrite in garnetite during retrograde metamorphism in the Curnamona Province adds evidence for coeval metamorphic events recorded in the Western Fold Belt of the Mount Isa Inlier and the Curnamona Province on the retrograde path.

Apparent closure temperatures of the Re-Os isotopic system in arsenopyrite

The blocking temperature of an isotope geochronometer in a given mineral species is a measure of its ability to retain primary age information through geologic and thermodynamic events. A minimum apparent closure temperature for the Re-Os arsenopyrite chronometer was conservatively estimated at 400 °C with the possibility of exceeding 450 °C (Morelli *et al*. 2010).

The only dynamothermal event that may have affected the arsenopyrite-löllingite-bearing garnetite rocks at Broken Hill is a Delamerian event with (1) temperatures of 530 to 600 °C localized in regional shear zones at 517 to 497 Ma (Dutch *et al*. 2005), and (2) a regional gradient up to ~350 °C at *ca*. 520 Ma (Harrison & McDougall 1981). Our Re-Os age for arsenopyrite corroborates petrographic observations in favor of arsenopyrite precipitation during retrograde metamorphism. This is consistent with closure of the Re-Os isotopic system during the Early Mesoproterozoic and its subsequent preservation once arsenopyrite had precipitated. Given that our garnetite sample was collected away from any Delamerian-age shear zones, our results imply that the Re-Os isotopic system was not disturbed by the ~350 °C Delamerian regional event. Our data confirm the proposal by Davies *et al*. (2010) and Morelli *et al*. (2010) for an estimate of closure temperature of the Re-Os isotopic system of *ca*. 400 to possibly 450 °C in arsenopyrite, *i.e*., the lower stability limit of arsenopyrite (400 to 550 °C; Pokrovski *et al*. 2002, Tomkins *et al*. 2006). By corollary, the preservation of the yet imprecise Re-Os age in löllingite (stability field of 625 to 550 °C) indicates that this Delamerian thermal event was not sufficient to reset the Re-Os isotopic system in löllingite either. In conclusion, our study supports the findings of Davies *et al*. (2010) and Morelli *et al*. (2010) that the potential for Re-Os dating in arsenopyrite and löllingite in high-grade metamorphic rocks is high, since the Re-Os systematics for these minerals do not appear to be readily disturbed by a later thermal event.

Rhenium concentrations in arsenopyrite and löllingite, possible source of Re, and Re-Os evidence for the origin of the Broken Hill deposit

Our Re-Os isotope study shows that löllingite can contain high proportions of Re (>320 ppb) and Os (>220,000 ppt) that are unusual for metallic minerals other than molybdenite (Freydier *et al*. 1997, Lambert *et al*. 1998, Stein *et al*. 1998, Ruiz & Mathur 1999, Mathur *et al*. 2000, Frick *et al*. 2001). Such Re and Os contents are particularly unusual in sediment-hosted ore systems (Tristá-Aguilera *et al*. 2006, Schneider *et al*. 2007) with the following two exceptions: (1) sulfide minerals in the Ruby Creek Cu deposit, Alaska, U.S.A. (*e.g*., Re in pyrite 525–2355 ppb, Re in chalcopyrite 80–3200 ppb, Re in bornite 1615–1700 ppb; Selby *et al*. 2009); (2) chalcopyrite and bornite from the Dzhezkazgan Cu deposit, Kazakhstan (*e.g*., Re in chalcopyrite 3.3–9.4 ppm, Re in bornite 8–10 ppm;

Box *et al*. 2012). Arsenopyrite in the garnetite sample from Broken Hill has extremely high Re (120 to 380 ppb) concentrations compared to the composition of arsenopyrite reported previously in the literature. For example, arsenopyrite from the Homestake gold deposit, South Dakota, contains ~3.5–63 ppb Re (Morelli *et al*. 2010), whereas that from the Three Bluffs gold deposit, Nunavut contains ~69–123 ppb Re (Davies *et al*. 2010). In contrast to the arsenopyrite from Homestake (total common Os contents of 3–21 ppt) and Three Bluffs (total common Os below 1.5 pg), for which the Os budget is almost exclusively composed of radiogenic ^{187}Os, arsenopyrite at Broken Hill has total common Os contents in the range of 24 to 255 ppb, thus diluting the budget of radiogenic ^{187}Os. Common Os was thus available in the source protolith for incorporation in arsenopyrite, and, by corollary, in earlier-formed löllingite.

Our results and observations lead us to the following interpretations and hypotheses: (1) arsenides like löllingite are natural sinks for Re and Os; (2) arsenopyrite, which formed from the destruction of löllingite, has unusually high Re contents that were inherited like other trace elements (*e.g*., Co, Ni, see above) during the breakdown of Re-rich löllingite; and (3) high Re contents in arsenide minerals such as löllingite might be explained by the fact that Re^{4+} forms diarsenides (*e.g*., similar to cubic sperrylite, $PtAs_2$) in which the oxidation state of arsenic is –2 (Szymanski 1979).

If the assertion of Spry & Wonder (1989), Plimer (2006), and Spry *et al*. (2007) that garnetite is the product of exhalite metamorphism is correct, then high concentrations of Re and Os in löllingite and arsenopyrite likely result from the concentration of Re and Os in these sulfarsenide minerals during metamorphism of the exhalite protolith. The initial ^{187}Os/^{188}Os ratio reflects the origin of bulk Os incorporated in a mineral at the time of precipitation prior to ingrowth of radiogenic ^{187}Os below the blocking temperature of the Re-Os system in this mineral (*e.g*., Walker *et al*. 1991). Löllingite and arsenopyrite have the same initial ^{187}Os/^{188}Os ratio of 0.66. Given that arsenopyrite formed at the expense of löllingite during retrograde metamorphism, this ratio reflects the origin of bulk Os incorporated in löllingite as it precipitated, and during conversion to arsenopyrite. Assuming that Os is sourced from exhalative sediments that formed at about 1680 Ma (*i.e*., the age of the Willyama Supergroup; Page *et al*. 2005a), we can back-calculate an estimate of the osmium isotopic composition of these sediments using the following equation (λ: decay constant of ^{187}Re; Smoliar *et al*. 1996; t = age of the Willyama Supergroup):

$$\left(^{187}\mathrm{Os}/^{188}\mathrm{Os}\right)_{\text{sediments}} = \left(^{187}\mathrm{Os}/^{188}\mathrm{Os}\right)_{\text{sulfarsenides}} - \left(^{187}\mathrm{Re}/^{188}\mathrm{Os}\right)_{\text{sediments}} * \left(e^{\lambda t} - 1\right)$$

If the exhalative sediments had a crustal ^{187}Re/^{188}Os signature of 34.5 (Peucker-Ehrenbrink & Jahn 2001), our estimate of the ^{187}Os/^{188}Os ratio of these sediments at 1680 Ma would be 0.59. This estimate is much higher than what is expected for a mantle source (^{187}Os/^{188}Os ~ 0.12), suggesting that the osmium source is, at least partially, of crustal origin. If the precursor to garnetite formed by the interaction of Mn-rich emanations from hydrothermal hot springs with pelagic clays (Spry & Wonder 1989), the initial ^{187}Os/^{188}Os ratio may reflect an original geochemical composition of evolved upper continental crust with an overprint of seawater in hydrothermal springs. The initial ratio falls within the lower range of ^{187}Os/^{188}Os ratios proposed for the upper continental crust (*cf*. Saal *et al*. 1998) for which the accepted (present-day) estimates of Re concentrations are 0.2 to 2 ppb Re (Sun *et al*. 2003).

Conclusions

Garnetite spatially associated with the Broken Hill Pb-Zn-Ag deposit, which was metamorphosed to the granulite facies, contains aggregates of sulfarsenide and sulfide minerals that consist of arsenopyrite and löllingite ± galena ± tetrahedrite interstitial to garnet crystals. The conclusions of our Re-Os isotope geochemistry and petrographic study are as follows:

Aggregates of arsenic-rich minerals consist of a core of black löllingite surrounded by dull grey arsenopyrite that contains unevenly distributed amounts of Co, Ni, and invisible, but detectable, gold as a result of the breakdown of löllingite. Petrographic observations are consistent with the destruction of löllingite and the redistribution of gold during retrograde metamorphism, as proposed by Tomkins & Mavrogenes (2001) for several arsenopyrite-bearing gold deposits.

Isochron regression of the Re-Os data points for arsenopyrite and arsenopyrite ± löllingite yields a Model 1 Re-Os age of 1574 ± 38 Ma (Early Mesoproterozoic). This age matches with the age of retrograde metamorphism (*ca*. 1590 to 1575 Ma) in the Broken Hill Block following peak granulite-facies metamorphic conditions at *ca*. 1602 Ma identified by SHRIMP U-Pb ages of monazite in garnetite (McFarlane & Frost 2009). Isochron regression of the Re-Os data points for löllingite and löllingite ± arsenopyrite yields an imprecise Model 1 age of 1707 ± 290 Ma that overlaps within error with the age of the arsenopyrite.

The arsenopyrite Re-Os age is consistent with an extended connection between the Olarian orogeny in the Broken Hill Block and the Isan orogeny in the Mount Isa area for which two distinct retrograde metamorphic events occurred at *ca*. 1575 Ma and *ca*. 1532 Ma.

Arsenopyrite and löllingite have unusually high concentrations of Re and Os for metallic minerals other than molybdenite. An initial $^{187}Os/^{188}Os$ ratio of 0.66 determined through regression of Re-Os data is common to the isochrons of löllingite data points on the one hand and arsenopyrite ones on the other hand. This initial ratio is compatible with a calculated original ratio of 0.59 in the sediments of the Willyaman Supergroup at *ca*. 1680 Ma, thereby indicating a, at least partially, crustal source of Os. By corollary, considering that the garnetite formed with this initial $^{187}Os/^{188}Os$ ratio, this may illustrate an original geochemical composition of an evolved upper continental crust with overprint of seawater in hydrothermal springs, a scenario compatible with the model of interaction of Mn-rich emanations from hydrothermal hot springs with pelagic clays in the long-lived Broken Hill Block (Spry & Wonder 1989). We propose that Re disseminated in the original Mn-rich exhalite protolith was concentrated in the sulfarsenide phases during granulite-facies metamorphism.

The Early Mesoproterozoic Re-Os age of arsenopyrite was retained despite a regional thermal event (350 °C and *ca*. 5 kbar) at *ca*. 520 Ma during the Delamerian orogeny. Our study favors the conservative estimate of 400 °C for the closure temperature of the Re-Os isotope system in arsenopyrite (Davies *et al*. 2010, Morelli *et al*. 2010).

The current study supports the conclusion of Davies *et al*. (2010) and Morelli *et al*. (2010) regarding the potential for Re-Os dating using arsenopyrite and löllingite that would have preserved original age information of high-grade metamorphic events, in particular in thermally long-lived Precambrian cratonic provinces.

Acknowledgments

This research was supported by the Swiss National Science Foundation (Swiss NSF) through an Early Postdoc Mobility Grant (#P2GEP2_162075) awarded to N.J. Saintilan, and an NSERC Discovery Grant awarded to R.A. Creaser. Mark Simms is thanked for assistance in mineral processing, whereas Diane Caird ran XRD analyses at the University of Alberta. We thank Dr. Rafael del Rio and two anonymous reviewers for their detailed and pertinent reviews that contributed to greatly improve and clarify the manuscript. The work by Editor Dr. Lee A. Groat and Associate Editor Dr. Antoni Camprubí is acknowledged.

References

Binns, R.A. (1964) Zones of progressive regional metamorphism in the Willyama Complex, Broken Hill district, New South Wales. *Journal of the Geological Society of Australia* **11**, 283–330.

Box, S.E., Syusyura, B., Seltmann, R., Creaser, R.A., Dolgopolova, A., & Zientek, M.L. (2012) Dzhezkazgan and associated sandstone copper deposits of the Chu-Sarysu basin, Central Kazakhstan. *Economic Geology Special Publication* **16**, 303–328.

Connors, K.A. & Page, R.W. (1995) Relationships between magmatism, metamorphism and deformation in the western Mount Isa Inlier, Australia. *Precambrian Research* **71**, 131–153.

Corbett, G.J. & Phillips, G.N. (1981) Regional retrograde metamorphism of a high grade terrain: the Willyama Complex, Broken Hill, Australia. *Lithos* **1**, 59–73.

Creaser, R.A., Papanastassiou, D.A., & Wasserburg, G.J. (1991) Negative thermal ion mass spectrometry of osmium, rhenium and iridium. *Geochimica et Cosmochimica Acta* **55**, 396–401.

Davies, T., Richards, J.P., Creaser, R.A., Heaman, L.M., Chacko, T., Simonetti, A., Williamson, J., & McDonald, D.W. (2010) Paleoproterozoic age relationships in the Three Bluffs Archean iron formation-hosted gold deposit, Committee Bay Greenstone Belt, Nunavut, Canada. *Exploration and Mining Geology* **19**, 55–80.

Dutch, R.A., Hand, M., & Clark, C. (2005) Cambrian reworking of the southern Australian Proterozoic Curnamona Province: constraints from regional shear-zone systems. *Journal of the Geological Society of London* **162**, 763–775.

Ehlers, K., Foster, J., Nutman, A.P., & Giles, D. (1996) New constraints on Broken Hill geology and mineralisation. *In* New Developments in Broken Hill Type Deposits (J. Pongratz & G. Davidson, eds.). *CODES Special Publication* **1** (73–76).

Forbes, C.J., Betts, P.G., Giles, D., & Weinberg, R. (2008) Reinterpretation of the tectonic context of high-temperature metamorphism in the Broken Hill Block, NSW, and implications on the Palaeo- to Meso-Proterozoic evolution. *Precambrian Research* **166**, 338–349.

Freydier, C., Ruiz, J., Chesley, J., McCandless, T., & Munizaga, F. (1997) Re-Os isotope systematic of sulfides from felsic igneous rocks: Application to base metal porphyry mineralization in Chile. *Geology* **25**, 775–778.

Frick, L.R., Lambert, D.D., & Hoatson, D.M. (2001) Re-Os dating of the Radio Hill Ni-Cu deposit, west Pilbara

craton, Western Australia. *Australian Journal of Earth Sciences* **48**, 43–47.

Frost, B.R., Mavrogenes, J.A., & Tomkins, A.G. (2002) Partial melting of sulfide ore deposits during medium- and high-grade metamorphism. *Canadian Mineralogist* **40**, 1–18.

Frost, B.R., Swapp, S.M., & Gregory, R.W. (2005) Prolonged existence of sulfide melt in the Broken Hill orebody, New South Wales, Australia. *Canadian Mineralogist* **43**, 479–494.

Giles, D., Betts, P.G., & Lister, G.S. (2004) 1.8–1.5 Ga links between the North and South Australian Cratons and the Early-Middle Proterozoic configuration of Australia. *Tectonophysics* **380**, 27–41.

Hand, M. & Rubatto, D. (2002) The scale of the thermal problem in the Mount Isa inlier. *Geological Society of Australia Abstracts* **67**, 173.

Hand, M., Rutherford, L., & Barovich, K. (2003) Garnet Sm-Nd age constraints on the timing of tectonism in the southwestern Curnamona Province: implications for existing models and correlations. *Geoscience Australia Record* **13**, 65–68.

Harrison, T.M. & McDougall, I. (1981) Excess ^{40}Ar in metamorphic rocks from Broken Hill, New South Wales: implications for ^{40}Ar/^{39}Ar age spectra and the thermal history of the region. *Earth and Planetary Science Letters* **55**, 123–149.

Hnatyshin, D., Kontak, D.J., Turner, E.C., Creaser, R.A., Morden, R., & Stern, R.A. (2016) Geochronologic (Re-Os) and fluid-chemical constraints on the formation of the Mesoproterozoic-hosted Nanisivik Zn-Pb deposit, Nunavut, Canada: Evidence for early diagenetic, low-temperature conditions of formation. *Ore Geology Reviews* **79**, 189–217.

Hodgson, C.J. (1975) The geology and geological development of the Broken Hill lode in the New Broken Hill Consolidated Mine, Australia. Part III: Petrology and petrogenesis. *Journal of the Geological Society of Australia* **22**, 195–214.

Kretschmar, U. & Scott, S.D. (1976) Phase relations involving arsenopyrite in the system Fe-As-S and their applications. *Canadian Mineralogist* **14**, 364–386.

Laing, W.P. & Beardsmore, T.J. (1986) Stratigraphic rationalization of the Eastern Mount Isa Block, recognition of key correlations with Georgetown and Broken Hill Blocks in an eastern Australian Proterozoic terrain, and their metallogenic implications. *Geological Society of Australia Abstracts* **15**, 114–115.

Laing, W.P., Majoribanks, R.W., & Rutland, R.W.R. (1978) Structure of the Broken Hill Mine area and its significance for the genesis of the orebodies. *Economic Geology* **73**, 1112–1136.

Lambert, D.D., Foster, J.G., Frick, L.R., Hoatson, D.M., & Purvis, A.C. (1998) Application of the Re-Os isotopic system to the study of Precambrian sulfide deposits of Western Australia. *Australian Journal of Earth Sciences* **45**, 265–284.

Lottermoser, B.G. (1989) Rare earth element study of exhalites within the Willyama Supergroup, Broken Hill Block, Australia. *Mineralium Deposita* **24**, 92–99.

Ludwig, K.R. (2011) *User's manual for Isoplot 4.15: A geochronological toolkit for Microsoft Excel*. Berkeley Geochronology Center, Berkeley, California, U.S.A.

MacCready, T., Goleby, B.R., Goncharov, A., Drummond, B.J., & Lister, G.S. (1998) A framework of overprinting orogens based on interpretation of the Mount Isa deep seismic transect. *Economic Geology* **93**, 1422–1434.

Majoribanks, R.W., Rutland, R.W.R., Glen, R.A., & Laing, W.P. (1980) The structure and tectonic evolution of the Broken Hill region, Australia. *Precambrian Research* **13**, 209–240.

Mathur, R., Ruiz, J., & Munizaga, F. (2000) Relationship between copper tonnage of Chilean base-metal porphyry deposits and Os isotope ratios. *Geology* **28**, 555–558.

McFarlane, C.R.M. & Frost, B.R. (2009) Constraints on the early metamorphic evolution of Broken Hill, Australia, from in situ U-Pb dating and REE geochemistry of monazite. *Journal of Metamorphic Geology* **27**, 3–17.

Mezger, K., Essene, E.J., & Halliday, A.N. (1992) Closure temperatures of the Sm-Nd system in metamorphic garnets. *Earth and Planetary Science Letters* **113**, 397–409.

Morelli, R.M., Bell, C.C., Creaser, R.A., & Simonetti, A. (2010) Constraints on the genesis of gold mineralization at the Homestake Gold Deposit, Black Hils, South Dakota from Re-Os sulfide geochronology. *Mineralium Deposita* **45**, 461–480.

Page, R.W. & Laing, W.P. (1992) Felsic metavolcanics rocks related to the Broken Hill Pb-Zn-Ag orebody, Australia: Geology, depositional age and timing of high-grade metamorphism. *Economic Geology* **87**, 2138–2168.

Page, R.W., Conor, C.H.H., Stevens, B.P.J., Gibson, G.M., Preiss, W.V., & Southgate, P.N. (2005a) Correlation of Olary and Broken Hill Domains, Curnamona Province: Possible Relationship to Mount Isa and Other North Australian Pb-Zn-Ag-Bearing Successions. *Economic Geology* **100**, 663–676.

Page, R.W., Stevens, B.P.J., & Gibson, G.M. (2005b) Geochronology of the sequence hosting the Broken Hill Pb-Zn-Ag orebody. *Economic Geology* **100**, 633–661.

Peucker-Ehrenbrink, B. & Jahn, B.-M. (2001) Rhenium-osmium isotope systematic and platinum group element

concentrations: Loess and the upper continental crust. *Geochemistry, Geophysics, and Geosystems* **2**, 2001GC000172.

Phillips, G.N. (1980) Water activity changes across an amphibolites-granulite facies transition, Broken Hill, Australia. *Contributions to Mineralogy and Petrology* **75**, 377–386.

Phillips, G.N. & Wall, V.J. (1981) Evaluation of prograde regional metamorphic conditions: their implications for the heat source and water activity during metamorphism in the Willyama Complex. *Bulletin de Minéralogie* **104**, 801–810.

Plimer, I.R. (2006) Manganoan garnet rocks associated with the Broken Hill Pb-Zn-Ag orebody, Australia. *Mineralogy and Petrology* **88**, 443–478.

Pokrovski, G.S., Kara, S., & Roux, J. (2002) Stability and solubility of arsenopyrite, FeAsS, in crustal fluids. *Geochimica et Cosmochimica Acta* **66**, 2361–2378.

Prendergast, K., Stansfield, S., & Williams, P.J. (1998) Syn-late tectonic metasomatism in Western A-lode, Broken Hill. *Geological Society of Australia Abstracts* **49**, 364.

Raič, S., Mogessie, A., Benko, Z., Molnar, F., Hauck, S., & Severson, M. (2014) Arsenic-enriched Cu-Ni-PGE mineralization in Wetlegs, Duluth Complex, St. Louis County, Minnesota, USA. European Geosciences Union General Assembly 2014, 27 April–2 May 2014, Vienna, Austria, 3324.

Ruiz, J. & Mathur, R. (1999) Metallogenesis in continental margins: Re-Os evidence from porphyry copper deposits in Chile. *Reviews in Economic Geology* **12**, 59–72.

Saal, A.E., Rudnick, R.L., Ravizza, G.E., & Hart, S.R. (1998) Re-Os isotope evidence for the composition, formation and age of the lower continental crust. *Nature* **397**, 58–61.

Schneider, J., Melcher, F., & Brauns, M. (2007) Concordant ages for the giant Kipushi base metal deposit from direct Rb-Sr and Re-Os dating of sulfides. *Mineralium Deposita* **42**, 791–797.

Selby, D., Kelley, K.D., Hitzman, M.W., & Zieg, J. (2009) Re-Os sulfide (bornite, chalcopyrite, and pyrite) systematics of the carbonate-hosted copper deposits at Ruby Creek, southern Brooks Range, Alaska. *Economic Geology* **104**, 437–444.

Sharp, Z.D., Essene, E.J., & Kelly, W.C. (1985) A re-examination of the arsenopyrite geothermometer: Pressure considerations and applications to natural assemblages. *Canadian Mineralogist* **23**, 517–534.

Smoliar, M.I., Walker, R.J., & Morgan, J.W. (1996) Re-Os ages of Group IIA, IIIA, IVA and IVB iron meteorites. *Science* **271**, 1099–1102.

Sparks, H.A. & Mavrogenes, J.A. (2003) Evidence in support of sulfide partial melting at Broken Hill, Australia. *In* Mineral Exploration and Sustainable Development (D.G. Eliopoulos, ed.). Millpress, Rotterdam, Netherlands (1027–1029).

Spry, P.G. (1978) *The geochemistry of garnet-rich lithologies associated with the Broken Hill orebody, N.S.W., Australia*. Unpublished M.Sc. Thesis, University of Adelaide, Australia, 129 pp.

Spry, P.G. & Wonder J.D. (1989) Manganese-rich garnet rocks associated with the Broken Hill Pb-Zn-Ag deposit, New South Wales, Australia. *Canadian Mineralogist* **27**, 275–292.

Spry, P.G., Heimann, A., Messerly, J., & Houk, R.S. (2007) Discrimination of metamorphic and metasomatic processes at the Broken Hill Pb-Zn-Ag deposit, Australia: Rare earth element signatures of garnet-rich rocks. *Economic Geology* **102**, 471–494.

Stein, H.J., Sundblad, K., Markey, R.J., Morgan, J.W., & Motuza, G. (1998) Re-Os ages for Archean molybdenite and pyrite, Kuittila-Kivisuo, Finland, and Proterozoic molybdenite, Kabeliai, Lithuania: Testing the chronometer in a metamorphic and metasomatic setting. *Mineralium Deposita* **33**, 329–345.

Stevens, B.P.J. (1986) Post depositional history of the Willyama Supergroup in the Broken Hill Block, New South Wales, Australia. *Australian Journal of Earth Sciences* **33**, 73–98.

Sun, W., Bennett, V.C., Eggins, S.M., Kamenetsky, V.S., & Arculus, R.J. (2003) Enhanced mantle-to-crust rhenium transfer in undegassed arc magmas. *Nature* **422**, 294–297.

Szymanski, J.T. (1979) The crystal structure of plararsite, Pt(As,S), and a comparison with sperrylite, $PtAs_2$. *Canadian Mineralogist* **17**, 117–123.

Tomkins, A.G. & Mavrogenes, J.A. (2001) Redistribution of gold within arsenopyrite and loellingite during pro- and retrograde metamorphism: Application to timing of mineralization. *Economic Geology* **96**, 525–534.

Tomkins, A.G. & Mavrogenes, J.A. (2002) Mobilization of gold as polymetallic melt during pelite anatexis at the Challenger deposit, south Australia: A metamorphosed Archean gold deposit. *Economic Geology* **97**, 1249–1271.

Tomkins, A.G., Frost, B.R., & Pattison, D.R.M. (2006) Arsenopyrite melting during metamorphism of sulfide ore deposits. *Canadian Mineralogist* **44**, 1045–1062.

Tristá-Aguilera, D., Barra, F., Ruiz, J., Morata, D., Talavera-Mendoza, O., Kojima, S., & Ferraris, F. (2006) Re-Os isotope systematics for the Lince-Estefanía deposit: Constraints on the timing and source of copper mineralization in a stratabound copper deposit, Coastal Cordillera of northern Chile. *Mineralium Deposita* **41**, 99–105.

VAUGHAN, J.P. & STANTON, R.L. (1984) Stratiform Pb-Zn mineralization in the Kuridala Formation and Soldiers Cap Group, Mount Isa Block, NW Queensland Anonymous. *Conference Series – Australian Institute of Mining and Metallurgy* **13**, 307–317.

VÖLKENING, J., WALCZYK, T., & HEUMANN, K. (1991) Osmium isotopic ratio determination by negative thermal ionization mass spectrometry. *International Journal of Mass Spectrometry and Ionic Physics* **105**, 147–159.

WALKER, R.J., MORGAN, J.W., NALDRETT, A.J., LI, C., & FASSETT, J.D. (1991) Re-Os isotope systematic of Ni-Cu sulfide ores, Sudbury Igneous Complex, Ontario: evidence for a major crustal component. *Earth and Planetary Science Letters* **105**, 416–429.

WRIGHT, J.V., HAYDON, R.C., & MCCONACHY, G.W. (1987) Sedimentary model for the giant Broken Hill Pb-Zn deposit. Australia. *Geology* **15**, 598–602.

Received May 2, 2016. Revised manuscript accepted December 13, 2016.